ADVANCED FUNCTIONAL MATERIALS

FULL PAPER

Photoluminescence and Electron Paramagnetic Resonance of ZnO Tetrapod Structures**

By *Aleksandra B. Djurišić*,* *Wallace C. H. Choy*, *Vellaisamy Arul Lenus Roy*, *Yu Hang Leung*, *Chung Yin Kwong*, *Kok Wai Cheah*, *Tumkur Krishnaswamy Gundu Rao*, *Wai Kin Chan*, *Hsian Fei Lui*, and *Charles Surya*

ZnO tetrapod nanostructures have been prepared by the evaporation of Zn in air (no flow), dry and humid argon flow, and dry and humid nitrogen flow. Their properties have been investigated using scanning electron microscopy (SEM), X-ray diffraction (XRD), photoluminescence (PL) and photoluminescence excitation (PLE) spectroscopies (at different temperatures), and electron paramagnetic resonance (EPR) spectroscopy at –160 °C and room temperature. It is found that the fabrication conditions significantly influence the EPR and PL spectra obtained. While a $g = 1.96$ EPR signal is present in some of the samples, green PL emission can be observed from all the samples. Therefore, the green emission in our samples does not originate from the commonly assumed transition between a singly charged oxygen vacancy and a photoexcited hole [K. Vanheusden, C. H. Seager, W. L. Warren, D. R. Tallant, J. A. Voigt, *Appl. Phys. Lett*. **1996**, *68*, 403]. However, the green emission can be suppressed by coating the nanostructures with a surfactant for all fabrication conditions, which indicates that this emission originates from surface defects.

1. Introduction

ZnO is of great interest for photonic applications due to its wide bandgap (3.37 eV) and large exciton binding energy (60 meV). The properties of ZnO have been studied extensively using various techniques, such as electron paramagnetic resonance,[1–19] positron annihilation spectroscopy,[20–26] and photoluminescence (PL).[2–6,20–22,27–58] Theoretical calculations investigating defects in ZnO have also been reported.[59–64] However, in spite of numerous studies on ZnO, there are still a number of unresolved issues on which contradictory explanations have been proposed, such as the nature of shallow donors in ZnO as well as the origin of the visible emission. Moreover, many contradictions in terms of the positions of reported peaks in EPR and PL and their assignment can be found in the literature. This is likely to be due to the large variation of the properties of ZnO depending on the fabrication conditions.

EPR is a useful tool for the investigation of the paramagnetic defects in the material. Lines in the EPR spectrum at $g = 2.0155$, $g = 2.0024$, and $g = 2.0165$ were attributed to the Zn vacancy.[7,8] EPR signals due to singly negatively charged Zn vacancy V_{Zn}^- and zinc vacancy–interstitial zinc complex V_{Zn}^-:Zn_i with g value close to 2 and interstitial oxygen O_i with $g_\perp = 1.9962$ and $g_\parallel = 1.9948$ were also reported.[15] EPR study of evolution of defects in ZnO during tribophysical activation revealed following features: $g = 2.019$ due to V_{Zn}^-:Zn_i centre, $g = 2.013$ due to V_{Zn}^-, $g = 2.0075$, $g = 2.0060$, and $g = 2.0015$ due two mutually close zinc vacancies which encompass one hole $(V_{Zn}^-)_2^-$, $g_\perp = 1.9965$ and $g_\parallel = 1.9950$ due to singly charged oxygen vacancy, and $g = 1.9640$ due to shallow donor centers.[13] A signal with $g = 2.003$ was attributed to chemisorbed O_2^-.[11,13] Two EPR studies on ZnO nanocrystallites found signals with $g = 2.0190$[12] and $g = 2.0106$[10] which was attributed to O^{2-} vacancies located at the surface of nanocrystallites. The location of defects at the surface was confirmed by reduction of EPR signal intensity by coating the particles with a layer of surfactant.[12] However, many EPR studies attribute the commonly observed signal $g = 1.96$ to the singly ionized oxygen vacancy V_O^+.[1,4–6,11,16,18]

Based on the correlation between the intensity of this EPR signal and the green PL intensity, green emission has been explained as the transition between a singly charged oxygen vacancy and a photoexcited hole.[4,5] This explanation has been commonly adopted in order to explain visible emission in ZnO single crystals,[29] thin films,[40] powders,[6] and nanostruc-

[*] Dr. A. B. Djurišić, Y. H. Leung
Department of Physics, The University of Hong Kong
Pokfulam Road (Hong Kong)
E-mail: dalek@hkusua.hku.hk
Dr. W. C. H. Choy, Dr. V. A. L. Roy, C. Y. Kwong
Department of Electrical & Electronic Engineering
University of Hong Kong
Pokfulam Road (Hong Kong)
Dr. K. W. Cheah
Department of Physics, Hong Kong Baptist University
Kowloon Tong (Hong Kong)
Dr. T. K. Gundu Rao
RSIC, Indian Institute of Technology, Mumbai (India)
Dr. W. K. Chan
Department of Chemistry, The University of Hong Kong
Pokfulam Road (Hong Kong)
H. F. Lui, Dr. C. Surya
Department of Electronic and Information Engineering
Hong Kong Polytechnic University
Hung Hom, Kowloon (Hong Kong)

[**] The authors would like to thank Amy Wong and Wing Song Lee for SEM measurements, and Dr. J. Gao for XRD measurements. This work is supported by the University Research Committee seed funding grant of the University of Hong Kong.

  DOI: 10.1002/adfm.200305082

ADVANCED FUNCTIONAL MATERIALS

tures.[47,50,52,54] Although originally proposed to explain broad green emission centered at 510 nm,[4,5] the oxygen-vacancy hypothesis was cited as an explanation of the peaks from 495 nm (in tetrapod ZnO nanorods)[50] to 583 nm (tubular ZnO whiskers).[44] However, the assignment of the $g = 1.96$ EPR signal to the singly ionized oxygen vacancy is a controversial issue. It was pointed out that V_o^+ produces the EPR signal $g_\perp = 1.9945$ and $g_\parallel = 1.9960$,[2,3,19] while the signal $g = 1.96$ is typically assigned to shallow donors[1–3,13,17] and its position appears to be independent on the shallow donor identity.[2] There are two possible intrinsic donors in ZnO: i) an oxygen vacancy and ii) interstitial zinc. According to some earlier works, both of these defects have similar properties and it is difficult to distinguish between them.[64] Morazzoni et al.[1] attributed two close EPR signals at $g = 1.955$ and $g = 1.958$ to Zn_i^+ and V_o^+, respectively. However, a study of electron-irradiated ZnO samples indicates that the native shallow donor in ZnO is interstitial Zn or the Zn_i-related complex.[65] Recent theoretical calculations indicate that Zn_i is the native shallow donor[62] and that the oxygen vacancy is a deep donor.[59–62] Also, recent experiments on the influence of the electric field with the green luminescence in ZnO single crystals indicate that the luminescence is due to complex defects including zinc interstitials.[66] However, it should be pointed out that the contradictory results have been reported for the calculations of the formation energies of the native defects in ZnO. While Zhang et al.[62] found that the formation enthalpy for Zn_i is low under both Zn-rich and O-rich conditions, other studies predicted that the oxygen vacancy has the lowest formation energy,[60,63] but cannot explain n-type conductivity in undoped ZnO since it is a deep donor.[60] From the electronic structure calculations, either zinc interstitial defects or zinc antisite defects were identified as possible native donors.[60]

Positron annihilation spectroscopy (PAS) was also used in order to study native defects in ZnO.[20–26] The majority of PAS studies found that the dominant types of defects were the zinc vacancy V_{Zn}^- or V_{Zn}-related complexes,[20–23] such as divacancy $V_{Zn}V_O$.[20,23] The presence of other types of defects, such as Zn; and oxygen vacancies were deduced from the diffusion length of the positrons.[22] However, proposed interpretations of the relationship between point defects that were detected by PAS and visible luminescence are different. Zhong et al.[23] found no direct relationship between positron lifetime and visible (yellow) luminescence, which was assigned to Zn vacancies that were trapped in grain boundaries. Liu et al.[20] reported that Mn doping does not change the concentration of defects detected by PAS but quenches visible luminescence. They concluded that PAS does not probe directly luminescent centers in ZnO. They proposed that green and yellow luminescence in ZnO are due to Zn_i and O_i, respectively.

In spite of a number of studies that were performed on the photoluminescence of ZnO, there is no consensus in the literature on the positions of the peaks in PL spectrum of ZnO nanostructures and thin films or their origin. In addition to the most commonly observed green luminescence, violet and blue luminescence from ZnO thin films, nanoparticles, and whiskers were reported before.[35,40,48,49,56–58] Among the peaks reported are 405 nm,[57] ~420 nm,[35,49,57,58] 446 nm,[56] 466 nm,[48] and ~485 nm.[49,57] Blue luminescence at 405 nm has been attributed to the zinc vacancy.[40] According to calculations, 405 nm transition corresponds to the Zn vacancy, 427 nm transition to interstitial zinc, and 544 nm to interstitial oxygen.[55] Blue emission at ~413 nm was observed in ZnO films that were grown under oxygen rich conditions, and it was attributed to the possible existence of cubic ZnO.[37] The emission at ~420 nm has been attributed to the interstitial oxygen,[49,58] transition between defects (interface traps) at grain boundaries and the valence band, and lattice defects that are related to oxygen and zinc vacancies[57] while the emission at 446 nm was attributed to the transition between shallow donor (oxygen vacancy) to the valence band.[56] A vague explanation (oxygen and zinc vacancies or interstitials and their complexes) was given for the 466 nm emission peak.[48] The 485 nm emission was attributed to a transition between the oxygen vacancy and interstitial oxygen[49] and lattice defects related to oxygen and zinc vacancies.[57] In addition to violet, blue, and green emissions from ZnO reported in the literature, red emission (640 nm) in ZnO thin films fabricated by spray pyrolysis was also reported.[31] Also, yellow emission (583 nm) from single-crystal tubular ZnO whiskers was reported.[44] The yellow emission has been assigned to interstitial oxygen[40] and the oxygen vacancy.[44]

It can be observed that the assignment of the transitions to observed peaks in the PL spectrum of ZnO samples is often contradictory. Out of reported PL emission peaks, the origin of commonly observed broad green or green–yellow emission is the most controversial. Several different emission mechanisms have been proposed, such as the transition between photoexcited holes and singly ionized oxygen vacancy,[4,5] copper impurities,[3,30] antisite oxygen,[55] surface states,[51] and donor–acceptor complexes.[32,39,42] It was also proposed that the transition from an electron in the conduction band to a deep acceptor is unlikely,[41] while the studies on nanocrystalline ZnO particles[45,46] indicate that the visible emission is due to the transition of an electron from a level close to conduction band to a deeply trapped hole in the bulk of ZnO nanoparticle. Therefore, it can be concluded that no consensus has been reached on the origin of the visible emission in ZnO.

In this work, we have used EPR, low-temperature and room temperature (RT) PL, and photoluminescence excitation (PLE) spectroscopies to study the luminescent properties of ZnO nanostructures (tetrapods and nanowire + tetrapod structures[67]) that are prepared under different conditions. We have found no obvious correlation between EPR signal and the visible luminescence. EPR line at $g = 1.96$ is present in some of the samples, but green photoluminescence is observed for all the samples including those which do not show EPR line at $g = 1.96$. Therefore, it is clear that the common hypothesis that the green emission in ZnO originates from transition between photoexcited hole and singly ionized oxygen vacancy does not represent a universal explanation of green emission in ZnO. Based on the results obtained in this work and the data reported in the literature, we conclude that the most likely explanation for green luminescence in ZnO involves multiple defects

and/or defect complexes. We also investigated whether the visible emission originates from the surface or from the bulk of the nanostructures, by coating the fabricated nanostructures with surfactant. A significant decrease in the visible PL after surfactant coating is indicative of the fact that the major part of the visible emission originates from centers at the nanostructure surface.

2. Results and Discussion

Figure 1 shows representative scanning electron microscopy (SEM) images of fabricated nanostructures. In air (no flow), tetrapod structures are obtained (see Fig. 1a), while in gas flow, regardless of type of the gas, a mixture of tetrapods and nanowires are obtained (see Fig. 1b). Figure 2 shows the X-ray diffraction (XRD) patterns for ZnO tetrapod nanorods that are fabricated in air. For all fabrication conditions, XRD data show peaks corresponding to wurtzite ZnO. No diffraction peaks from Zn or other impurities were detected.

In order to investigate the presence of paramagnetic defects, we performed EPR measurements at –160 °C and RT. Even though all the samples exhibited some emission in the visible spectral range, the commonly reported EPR signal with $g = 1.96$ was observed in only some of the samples. At –160 °C, the ZnO sample that was fabricated in air showed only a broad line with a linewidth of 465 gauss. The g value was found to be 2.0028. This is in good agreement with previously reported signal at $g = 2.003$ which was attributed to chemisorbed oxygen.[11,13] In samples that were fabricated under humid argon and humid nitrogen, a line with $g = 1.96$ can be observed in addition to a weak feature with g value 2.0049. The samples that were fabricated in dry argon and dry nitrogen flow did not exhibit any obvious EPR lines. At room temperature, as shown in Figure 3, only a very weak broad feature between $g \sim 2.00$ and $g \sim 2.05$ was observed. The samples fabricated in humid gas

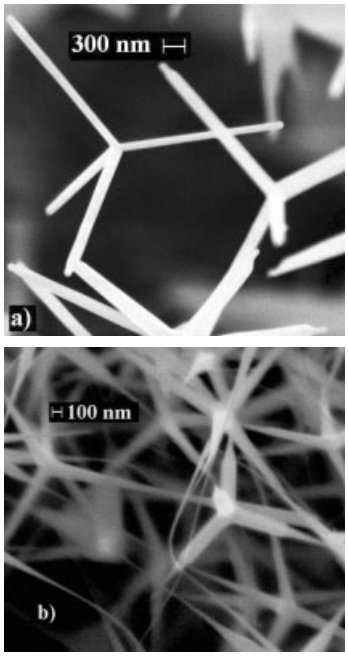

Figure 1. Representative SEM images of ZnO nanostructures a) in air (no flow) b) in humid argon flow.

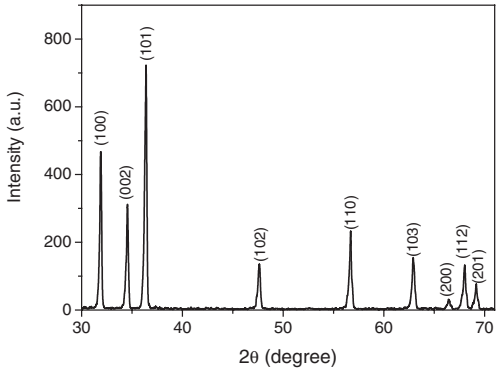

Figure 2. XRD pattern from ZnO tetrapod nanorods fabricated in air.

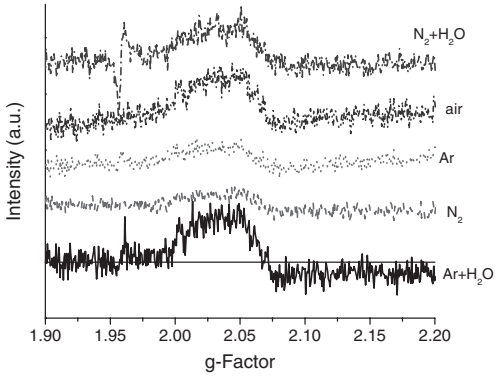

Figure 3. EPR spectra measured at room temperature from ZnO nanostructures prepared under different conditions.

flow (both argon and nitrogen) also showed a line at $g = 1.96$, which is more pronounced for the sample fabricated in humid nitrogen flow. Assignment of a weak feature at 2.0049 is not fully clear. EPR signals with peak values in the range from $g = 2.0015$ to $g = 2.0075$ have been attributed to a Zn vacancy,[7,8] two mutually close zinc vacancies which encompass one hole,[13] and chemisorbed oxygen.[68] Chemisorbed oxygen was reported to result in a very broad feature between $g \sim 2.007$ and $g \sim 2.05$,[68] which is in agreement with the broad peak that was observed in our RT EPR measurements. Therefore, we conclude that this broad feature is most likely due to the chemisorbed oxygen. This conclusion is supported with the fact that the intensity of this feature is lower in freshly fabricated samples than in the samples which have been exposed to atmosphere for two weeks. The signal with $g = 1.96$ is typically assigned to shallow donors.[1–3,13,17] It should be pointed out, however, that this signal is most likely not due to the oxygen vacancy.[2,3,19,69,70] Free electrons were also identified as the possible cause of $g = 1.96$ EPR signal.[70] Theoretical calculations predict that the singly charged oxygen vacancy is always higher in energy than both V_o and V_o^{2+}.[69] It is expected that the signal that was due to V_o^+ can be observed upon light excitation, so

ADVANCED FUNCTIONAL MATERIALS

that the assignment to a light-sensitive center with $g \sim 1.99$ is more likely.[69] Another argument in favor of the assignment of the $g = 1.99$ EPR signal to oxygen vacancy is the tetrahedral symmetry of the paramagnetic centre.[70]

Figures 4–8 show photoluminescence at different temperatures for ZnO nanostructures that are fabricated in air, dry argon, humid argon, dry nitrogen, and humid nitrogen, respectively. It can be observed that at 11 K in the UV region similar features can be observed for all five fabrication conditions. From the previously reported data on low temperature PL studies in ZnO films,[33,34,36] several narrow peaks due to free excitons, donor (ionized and neutral)-bound excitons, neutral acceptor-bound excitons and their two electron satellites and phonon replicas are expected. The peak positions at ~3.34 eV and ~3.30 eV are in very good agreement with previously reported results for ZnO films[36] and nanocrystalline ZnO films.[34] In addition to these two peaks, a peak at 3.22 eV can also be observed. This feature in ZnO films was assigned to donor–acceptor transition.[36] With the temperature increase, the excitonic peak becomes more broad and shifts to a lower energy, which is in very good agreement with the previously reported results for nanocrystalline ZnO films.[36] However, the peak shift is not equal for all the fabrication conditions, so that the samples fabricated in argon and humid nitrogen exhibit an ~8 nm shift compared to the sample prepared in air and a ~5 nm shift compared to the sample prepared in humid argon. For fabrication in dry nitrogen flow, the UV peak completely disappears at room temperature.

As for the emission in the visible spectral range, more significant differences between different preparation conditions can be observed. At room temperature, all the samples except the sample that was fabricated in dry argon flow exhibited a broad

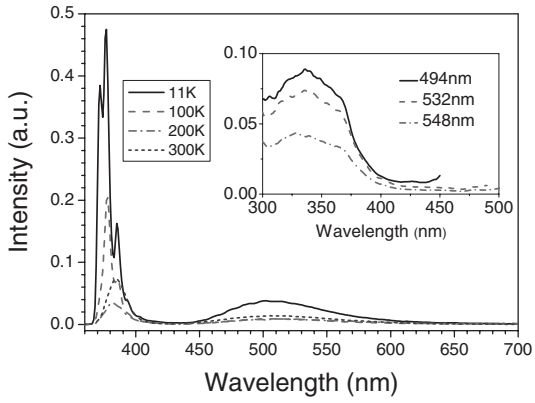

Figure 4. PL at different temperatures for ZnO nanostructures prepared in air. The inset figure shows the PLE spectrum for different wavelengths at 11 K.

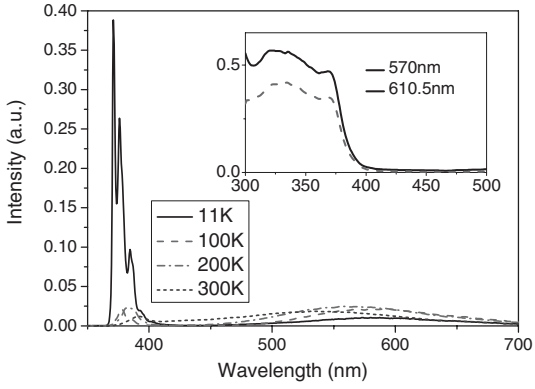

Figure 5. PL at different temperatures for ZnO nanostructures prepared in argon flow. The inset figure shows the PLE spectrum for different wavelengths at 11 K.

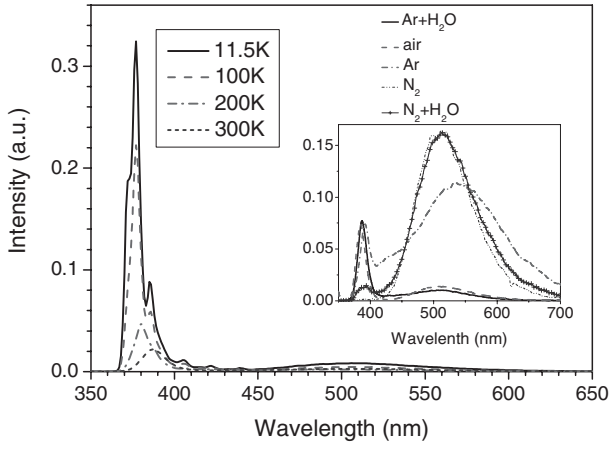

Figure 6. PL at different temperatures for ZnO nanostructures prepared in humid argon flow. The inset shows a comparison of room temperature photoluminescence for different atmospheres.

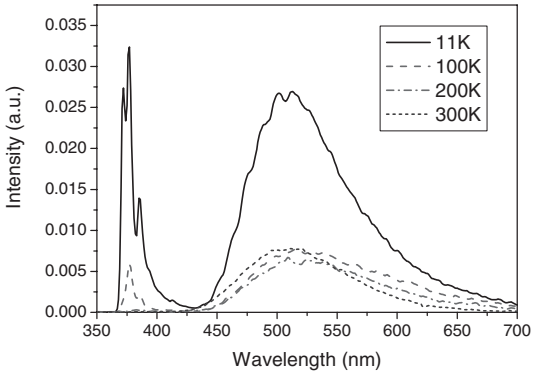

Figure 7. PL at different temperatures for ZnO nanostructures prepared in nitrogen flow.

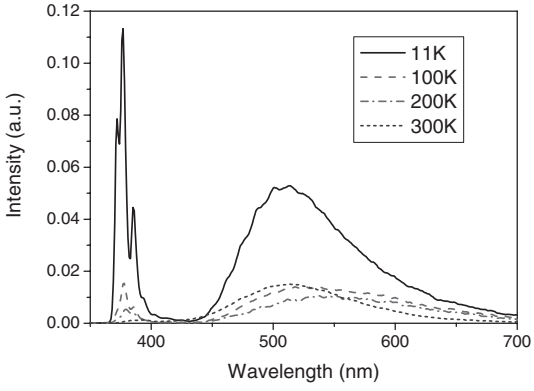

Figure 8. PL at different temperatures for ZnO nanostructures prepared in humid nitrogen flow.

peak that was centered at ~510 nm. The visible emission peak in the sample fabricated in argon flow exhibits some red-shift compared to the other samples. This is in agreement with previously reported results for sputtered ZnO films, where it was found that the visible PL from samples annealed in argon was dominated by yellow emission while those annealed in oxygen showed both green and yellow emission.[71] The visible emission for all samples can be fitted with two to three Gaussian peaks. This is in agreement with previously reported results for polycrystalline ZnO films, where visible emission was fitted with two Gaussian peaks, one in the green and one in the yellow spectral range.[27] We performed PLE measurements for fitted peak wavelengths at different temperatures. PLE curves at 11 K for samples that were grown in air and argon flow are shown in insets of Figures 4,5, respectively. Similar results are obtained for other samples and at other temperatures. No peaks are found above the bandgap of ZnO, indicating that there is no direct excitation of defect levels for either the green- nor the yellow-emission region. The samples fabricated in air and humid argon flow do not show any significant temperature-dependent shift in the green emission peak. The samples that were fabricated in dry argon flow exhibit a blue-shift of the visible emission peak with temperature, whilst samples that were fabricated in dry and humid nitrogen showed a small red-shift of the visible emission peak at 100 K and 200 K compared to the ~510 nm peak that was observed at 11 K and RT.

The comparison of PL at room temperature for samples that were fabricated under different conditions is shown in the inset of Figure 6 (the curves have been scaled for easier comparison). Since the samples are in powder form, it is difficult to ensure that same quantity is probed for different samples so that we cannot compare directly the emission intensity. However, we can compare the ratio of UV and visible emission as well as the peak position. It can be observed that the samples that are fabricated in air and humid argon flow show a strong UV emission and a similar UV-to-green emission ratio, with the sample that was fabricated in humid argon flow having slightly higher UV-to-green emission ratio. The sample fabricated under nitrogen flow does not show any significant UV emission at room temperature, while the sample that was fabricated under humid nitrogen flow showed weak UV emission. This is in agreement with the previously reported results that hydrogen-plasma irradiation[72] and annealing in H_2/Ar ambient[43] enhance UV emission in ZnO. This enhancement was attributed to passivation of deep donor and acceptor states by electron transfer from hydrogen to defects.[72] Hydrogen is expected to behave as a shallow donor in ZnO.[73] It should be noted that the samples that were fabricated under humid gas flow are the only samples that showed an EPR signal at $g = 1.96$ which is typically assigned to shallow donors.[13] Further investigation is needed before the exact origin of this signal can be established. While the samples that were prepared under different atmospheres exhibit different average sizes and morphologies, no significant shift of the defect emission peak relating to size was observed. Wood et al.[74] found a defect emission peak shift from blue to yellow for ZnO nanoparticles with sizes ranging from 1 nm to 6 nm. The difference between their results and the results reported here are likely to be due to the much larger sizes of the nanostructures that are fabricated by the evaporation reported in this work, as well as the differences in the fabrication method. For example, we have observed that ZnO nanorods (average diameter ~50 nm) that were fabricated from zinc nitrate hydrate and hexamethylenetetramine solution at 90 °C exhibited yellow rather than green photoluminescence, similar to larger ZnO nanoparticles.[74]

The samples that were fabricated in dry and humid argon flow exhibit one feature which is absent in other samples, namely that the PL emission does not fall to zero between the UV and broad visible emission peak, indicating a contribution from an additional transition in the range 400–450 nm. Emission in the blue spectral range for ZnO has been reported previously.[35,40,49,56–58] Possible candidates for transitions in this spectral range are zinc vacancy (405 nm),[40,55] interstitial zinc (427 nm),[55] and lattice defects related to oxygen and zinc vacancies (420 nm).[57] The peak at 420 nm was also attributed to interstitial oxygen,[49,58] but based on theoretical predictions[55,59] and other experimental results[20,40] it is more likely that interstitial oxygen is responsible for yellow emission. From the results obtained, it can be concluded that the gas flow has a significant influence on the type and concentration of the defects in ZnO nanostructures. Since the emission in the visible spectral range showed no correlation with the existence of EPR signal at $g = 1.96$, it can be concluded that the hypothesis that green emission was due to the singly charged oxygen vacancy proposed by Vanheusden et al.[4,5] is not applicable for our samples.

To further investigate the relationship between the existence of the $g = 1.96$ EPR signal and the green photoluminescence, we fabricated the samples in air with the same morphology (tetrapods, as shown in Fig. 1a) but from different starting material (ZnO from pure Zn at 950 °C and ZnO from the ZnO/graphite 1:1 mixture at 1100 °C). The obtained results are shown in Figure 9. It can be observed that the samples have a very similar ratio of UV-to-green emission, while the signifi-

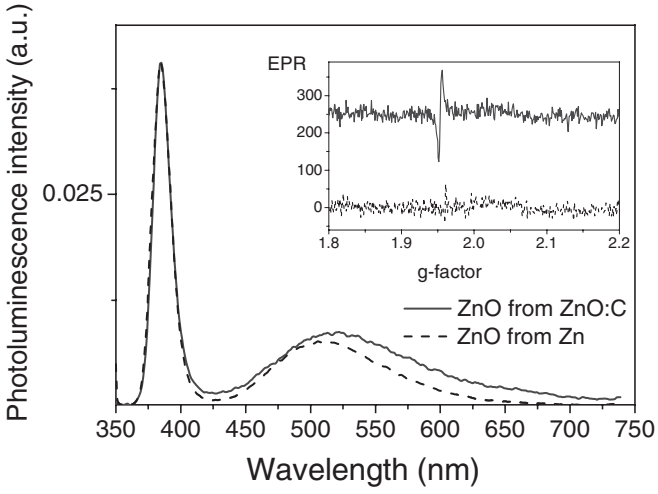

Figure 9. Photoluminescence of ZnO nanostructures prepared in air from Zn and ZnO/graphite (1:1) mixture. The inset shows corresponding EPR spectra.

ADVANCED FUNCTIONAL MATERIALS

cant $g = 1.96$ EPR signal is present only in the sample that was fabricated from ZnO:graphite mixture. The emission from the sample fabricated from ZnO:graphite mixture also shows a small red-shift of the emission. The origin of this shift is not fully clear, but one possible reason is that in one case we observe donor–acceptor transition in agreement with observations reported in the literature,[32,39,42] while in the other we see the transition between the electrons in the conduction band and the deep level. Further investigation is needed to conclusively establish mechanisms responsible for the observed phenomena. The $g = 1.96$ EPR signal actually can consist of two lines $g = 1.955$ and $g = 1.958$ which may be caused by different defects,[70] which further complicates the interpretation of the origins of transitions observed in the presence or absence of $g = 1.96$ EPR signal. It should also be noted that in this case the samples were characterized immediately after fabrication, so that the broad peak due to chemisorbed oxygen in the EPR spectrum is absent. The storage in vacuum at room temperature does not induce significant changes in the sample properties when the samples are stored immediately after fabrication. Effects of annealing in different atmospheres were not investigated due to the possible change in the size and morphology of the nanostructures.

Several other mechanisms for the green emission in ZnO have been proposed in the literature. Cu impurities have been proposed as the origin of the green emission in ZnO.[3,30] Garces et al.[3] proposed that the structured green emission (after high-temperature annealing) was associated with Cu^{2+} ions, while the unstructured emission that was observed before annealing was due to the donor–acceptor transition involving Cu^{+} acceptors. Donor–acceptor and shallow donor–deep level transitions have been proposed previously to explain the origin of green emission in ZnO.[28,32,39] However, there are several reasons why intrinsic defect are more likely to be responsible for green emission in our samples. Firstly, we found no evidence of the signal that was due to the Cu^{2+} ions in EPR measurements for our samples. Secondly, if the observed luminescence would be due to impurities in the starting material, the samples that were fabricated in the different gas flow would not exhibit such differences as those that were obtained here. Thirdly, the reported variation of the peak positions with different annealing conditions[27,43] and measured at different temperature[43] is more consistent with intrinsic defects than an extrinsic impurity. Also, the visible emission in ZnO is very broad, which cannot be explained by the width of impurity levels.[28] Therefore, while the emission due to copper impurities is possible in some ZnO samples, it is not likely that copper impurities are a universal explanation for green emission in ZnO. It should also be pointed out that our samples fabricated in nitrogen flow exhibit structured green emission at low temperature which Garces et al.[3] attribute to Cu^{2+} impurities while Reynolds et al.[39] attribute it to the transitions between the two shallow donors and acceptor, without identifying the donors and acceptor involved. Since these features are present only in samples that are fabricated in (both dry and humid) nitrogen flow and nitrogen is known to be an acceptor in ZnO[71] it is possible that observed features are due to the incorporation of nitrogen in our samples. Other donor–acceptor mechanisms that are proposed in the literature include transitions between an oxygen vacancy as a shallow donor and a zinc vacancy as an acceptor.[42] However, since the oxygen vacancy is a deep and not shallow donor,[59–62] this explanation is not likely. A neutral oxygen vacancy was also proposed as an explanation for green emission in ZnO.[29,62] Theoretical calculations typically place the oxygen vacancy level at 1.62–2.0 eV below the conduction band.[55,59,61] Another defect whose energy level corresponds to green emission is the antisite defect O_{Zn}, which is predicted to be 2.28 eV below the conduction band[55] or to have two levels 2.37 eV and 1.87 eV below the conduction band.[59] Another possible candidate for yellow–green emission is the O_2 acceptor which is predicted to be located 0.8 eV above the valence band.[61] It is known that chemisorbed oxygen at the ZnO surface forms surface acceptors.[75] van Dijken et al.[45,46] proposed that green emission involves trapping of holes by chemisorbed oxygen, followed by visible emission due to the transition of the electron from a shallow donor level to a deeply trapped hole (V_o^{**} center). Our EPR results indicate the presence of chemisorbed oxygen. However, no correlation is found between the intensity of the EPR signal assigned to chemisorbed oxygen and green PL intensity.

It should be pointed out that assigning the green emission to a single point defect[29,55,62] is in contradiction with the studies proposing donor–acceptor transitions.[28,32,39,42] Also, recent studies on the effect of electric field on the green luminescence in ZnO found that the emitting centers are complex defects involving Zn_i.[66] However, simple assignment of green and yellow luminescence to interstitial zinc and interstitial oxygen which was proposed previously[20] is not likely to be correct because the interstitial zinc is a shallow donor and the transition between Zn_i and the valence band could not produce green emission. The assignment of yellow emission to interstitial oxygen[20] is not in contradiction with predicted energy levels. While there are studies on the energy level of single point defects, theoretical works on energy levels of complex defects are scarce. Xu et al.[59] calculated the levels of various defects including complex defects V_o:Zn_i and V_{Zn}:Zn_i. They found no states within the gap from V_{Zn}:Zn_i, while for V_o:Zn_i two levels 1.2 eV and 2.4 eV above the valence band were found, so this type of defect represents a possible candidate for green emission in ZnO. The DLTS study of ZnO single crystals found a defect 0.59 eV below the conduction band with a high value of capture cross-section indicating that this defect may not be a simple point defect.[76] In addition to this unidentified defect, defects that were 0.10 eV, 0.12 eV, and 0.29 eV below the conduction band were found.[76]

We have also investigated the influence of excitation power and surface modifications to the ratio of UV and green emission in ZnO. Figure 10 shows the photoluminescence spectra of ZnO nanostructures that were grown in humid argon flow for different excitation powers. It can be observed that UV emission increases with the increase of excitation power, which is in agreement with the previously reported result for ZnO nanowires.[47] Saturation of green emission at low excitation intensity was attributed to the lower density of green emission

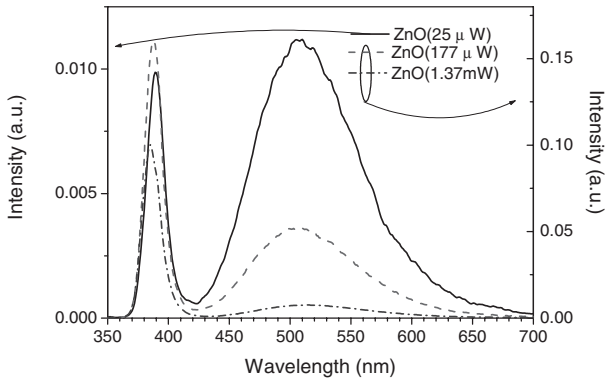

Figure 10. PL spectra for different excitation power for ZnO nanostructures prepared in humid argon flow.

centers compared to free excitons.[47] In order to establish whether the emission originates from defects on the surface or in the bulk, we have coated the fabricated nanostructures with surfactant (*n*-hexyltrichlorosilane) and compared the obtained PL spectra of ZnO nanostructures with and without surfactant, as shown in Figure 11. It can be observed that significant reduction in the green PL intensity is achieved with a surfactant, indicating that surface centers are involved. This is in agreement with previously reported results on reduction in the EPR signal with coating of ZnO nanocrystallites with surfactant[12] and the assignment of visible photoluminescence in ZnO nanoparticles to surface centers.[51] It has also been proposed that the green emission increases with the decrease in the size of ZnO nanowires since the surface to volume ratio increases.[52] However, it should be noted that the size of the nanostructures is temperature-dependent.[53] It was pointed out that the thinner ZnO nanowires grow in the low temperature region so that they are expected to have higher point defect density.[53] Since the defect density depends on the fabrication conditions, the relationship between nanostructure size and the green emission is more complex than the proposed simple rule smaller size = stronger green emission. Nevertheless, it is expected that the equilibrium concentrations of bulk defects are much smaller than concentrations of surface defects.[77] Therefore, it is very likely that the major part of the emission in the visible spectral range is due to defects located at the surface. A possible role of chemisorbed oxygen in visible luminescence, which was proposed previously,[45,46] cannot be entirely excluded here, but no direct relationship was found between EPR signal assigned to chemisorbed oxygen and visible PL intensity.

While it is at present not possible to conclusively establish the origin of green emission in ZnO, the results obtained here indicate that both the copper impurity and the singly ionized oxygen vacancy hypotheses can be excluded. The results reported in the literature and the results obtained in this work support the hypothesis that the emission is likely to involve multiple defects and/or defect complexes. The exact nature of these defects requires further study. Based on the large variation of the visible emission peaks that are reported in the literature, it is also possible that for different fabrication conditions different defects contribute to the visible emission. The results that are obtained also indicate that the concentration of green emission centers is lower than that of the free excitons, and, more importantly, that the majority of green emission centers are located at the surface of the nanostructures.

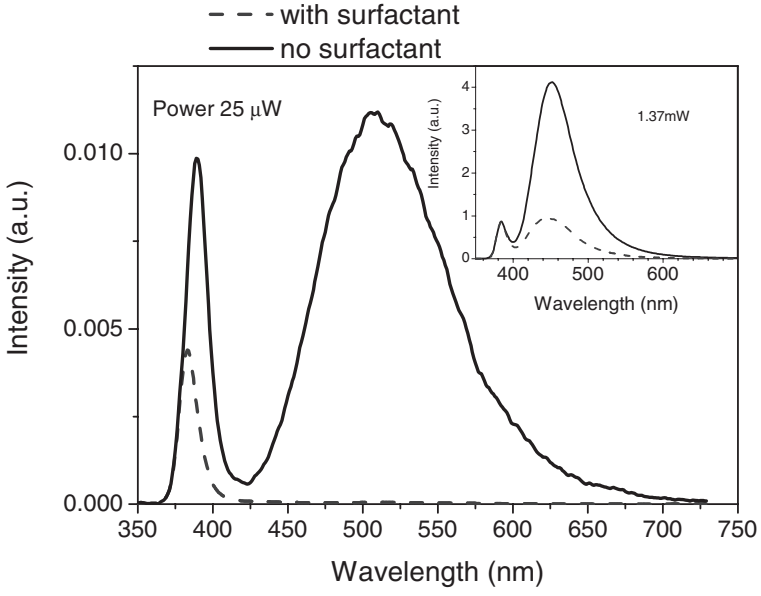

Figure 11. PL spectra of ZnO nanostructures fabricated in humid argon flow with and without surfactant for low power (50 μW) excitation. The inset shows PL spectra of ZnO nanostructures that are fabricated under nitrogen flow with and without surfactant for 1.37 mW excitation.

3. Conclusions

We have fabricated ZnO nanostructures in air, argon flow, humid argon flow, nitrogen flow, and humid nitrogen flow. Fabricated nanostructures were characterized using SEM, XRD, EPR, and temperature-dependent PL and PLE spectroscopies. It was found that, while the obtained morphologies were similar regardless of the gas flow, the type of gas had a significant influence on the EPR and PL results obtained. Unlike the previously reported studies on the ZnO powder which found a correlation between the EPR signal $g = 1.96$ and green luminescence for ZnO phosphor powders, no correlation was found in our ZnO tetrapod nanostructure samples. Only two of the samples exhibited a peak at $g = 1.96$ while all the samples showed luminescence in the visible region. The sample fabricated in humid argon flow exhibited low green luminescence and a peak at $g = 1.96$ while the sample that was fabricated in nitrogen flow showed a strong green luminescence and no EPR signal. Therefore, green luminescence probably originates from some non-paramagnetic defects or defect

ADVANCED FUNCTIONAL MATERIALS

complexes. Since the green emission can be significantly reduced by coating the nanostructures with surfactant, the major part of green emission originates from surface defects.

4. Experimental

The synthesis of ZnO nanostructures was performed as described previously [67]. Zn powder was evaporated in a quartz tube at 950 °C. The quartz tube was inserted into a horizontal tube furnace after the furnace had reached the desired temperature. For Ar and N_2 flow, a gas flow at a rate of 0.7 L min^{-1} was established. For deposition in humid gas flow, the gas was passed through water before being introduced into the furnace. In all cases, except dry nitrogen flow, which yielded mixture of white and gray products, white deposition products were obtained. The structure of deposited materials was investigated by X-ray diffraction (XRD) using a Siemens D5000 X-ray diffractometer and scanning electron microscopy (SEM) using a Cambridge-440 SEM. EPR measurements at –160 °C were performed using a Varian E-112 E-line Century Series X-band EPR spectrometer. TCNE ($g = 2.00277$) was used as a reference standard for *g*-factor measurements. Room-temperature EPR measurements were performed using a Bruker EMX EPR Spectrometer.

A He–Cd laser with 325 nm line was used as the excitation source for PL measurement. The beam was focused to the sample and the emitted light was collected into a double monochromator. The light was then detected by a PMT with response time of ~1 ns. The sample was placed in a cryostat such that the measurement can be carried out at 1×10^{-5} mbar and the temperature was cooled down to 11 K. For the PL excitation measurement, 1000 W Xe Arc lamp was used as excitation source. For investigating whether the emission originated from surface defects or not, fabricated nanostructures were coated with a surfactant using following procedure. ZnO nanostructures were dispersed in a dichloromethane solution of *n*-hexyltrichlorosilane in an ultrasonic bath for 1 h. After dispersion, nanostructures were separated using a centrifuge and rinsed thoroughly with dichloromethane to remove any residual surfactant and dried in an oven.

Received: October 9, 2003
Final version: February 16, 2004

[1] F. Morazzoni, R. Scotti, P. Di Nola, C. Milani, D. Narducci, *J. Chem. Soc., Faraday Trans.* **1992**, *88*, 1691.
[2] N. Y. Garces, N. C. Giles, L. E. Halliburton, G. Cantwell, D. B. Eason, D. C. Reynolds, D. C. Look, *Appl. Phys. Lett.* **2002**, *80*, 1334.
[3] N. Y. Garces, L. Wang, L. Bai, N. C. Giles, L. E. Halliburton, G. Cantwell, *Appl. Phys. Lett.* **2002**, *81*, 622.
[4] K. Vanheusden, C. H. Seager, W. L. Warren, D. R. Tallant, J. A. Voigt, *Appl. Phys. Lett.* **1996**, *68*, 403.
[5] K. Vanheusden, W. L. Warren, C. H. Seager, D. R. Tallant, J. A. Voigt, B. E. Gnade, *J. Appl. Phys.* **1996**, *79*, 7983.
[6] J. Koudelka, J. Horák, P. Jariabka, *J. Mater. Sci.* **1994**, *29*, 1497.
[7] D. Galland, A. Herve, *Solid State Commun.* **1974**, *14*, 953.
[8] D. Galland, A. Herve, *Phys. Lett. A* **1970**, *33*, 1.
[9] N. Ohashi, T. Nakata, T. Sekiguchi, H. Hosono, M. Mizuguchi, T. Tsurumi, J. Tanaka, H. Haneda, *Jpn. J. Appl. Phys., Part 2* **1999**, *38*, L113.
[10] L. Jing, Z. Xu, J. Shang, X. Sun, W. Cai, H. Guo, *Mater. Sci. Eng.* **2002**, *A332*, 356.
[11] A. B. Walters, B.-K. Na, C.-C. Liu, M. A. Vannice, *J. Mol. Catal. A: Chem.* **2000**, *162*, 287.
[12] B. Yu, C. Zhu, F. Gan, Y. Huang, *Mater. Lett.* **1998**, *33*, 247.
[13] N. G. Kakazev, T. V. Sreckovic, M. M. Ristic, *J. Mater. Sci.* **1997**, *32*, 4619.
[14] W. E. Carlos, E. R. Glaser, D. C. Look, *Physica B* **2001**, *308–310*, 976.
[15] A. Pöppl, G. Völkel, *Phys. Status Solidi A* **1991**, *125*, 571.
[16] P. H. Kasai, *Phys. Rev.* **1963**, *130*, 989.
[17] H. Zhou, A. Hofstaetter, D. M. Hofmann, B. K. Meyer, *Microelectron. Eng.* **2003**, *66*, 59.
[18] A. Pöppl, G. Völkel, *Phys. Status Solidi A* **1989**, *115*, 247.
[19] J. M. Smith, W. E. Vehse, *Phys. Lett. A* **1970**, *31*, 147.
[20] M. Liu, A. H. Kitai, P. Mascher, *J. Lumin.* **1992**, *54*, 35.
[21] T. Koida, S. Chichibu, A. Uedono, A. Tsukazaki, M. Kawasaki, T. Sota, Y. Segawa, H. Koinuma, *Appl. Phys. Lett.* **2003**, *82*, 532.
[22] A. Uedono, T. Koida, A. Tsukazaki, M. Kawasaki, Z. Q. Chen, S. F. Chichibu, H. Koinuma, *J. Appl. Phys.* **2003**, *93*, 2481.
[23] J. Zhong, A. H. Kitai, P. Mascher, W. Puff, *J. Electrochem. Soc.* **1993**, *140*, 3644.
[24] R. M. de la Cruz, R. Pareja, R. González, L. A. Boatner, Y. Chen, *Phys. Rev. B* **1992**, *45*, 6581.
[25] W. Puff, S. Brunner, P. Mascher, A. G. Balogh, *Mater. Sci. Forum* **1995**, *196–201*, 333.
[26] S. Brunner, W. Puff, A. G. Balogh, P. Mascher, *Mater. Sci. Forum* **2001**, *363–365*, 141.
[27] Y. G. Wang, S. P. Lau, H. W. Lee, S. F. Yu, B. K. Tay, X. H. Zhang, H. H. Hng, *J. Appl. Phys.* **2003**, *94*, 354.
[28] D. C. Reynolds, D. C. Look, B. Jogai, H. Morkoç, *Solid State Commun.* **1997**, *101*, 643.
[29] F. H. Leiter, H. R. Alves, A. Hofstaetter, D. M. Hofmann, B. K. Meyer, *Phys. Status Solidi B* **2001**, *226*, R4.
[30] R. Dingle, *Phys. Rev. Lett.* **1969**, *23*, 579.
[31] S. A. Studenikin, N. Golego, M. Cocivera, *J. Appl. Phys.* **1998**, *84*, 2287.
[32] S. A. Studenikin, M. Cocivera, *J. Appl. Phys.* **2002**, *91*, 5060.
[33] S. A. Studenikin, M. Cocivera, W. Kellner, H. Pascher, *J. Lumin.* **2000**, *91*, 223.
[34] X. T. Zhang, Y. C. Liu, Z. Z. Zhi, J. Y. Zhang, Y. M. Lu, D. Z. Shen, W. Xu, X. W. Fan, X. G. Kong, *J. Lumin.* **2002**, *99*, 149.
[35] B. J. Jin, S. Im, S. Y. Lee, *Thin Solid Films* **2000**, *366*, 107.
[36] K. Thonke, Th. Gruber, N. Teofilov, R. Schönfelder, A. Waag, R. Sauer, *Physica B* **2001**, *308–310*, 945.
[37] T. Sekiguchi, K. Haga, H. Inaba, *J. Cryst. Growth* **2000**, *214/215*, 68.
[38] K. Ogata, K. Sakurai, Sz. Fujita, Sg. Fujita, K. Matsushige, *J. Cryst. Growth* **2000**, *214/215*, 312.
[39] D. C. Reynolds, D. C. Look, B. Jogai, *J. Appl. Phys.* **2001**, *89*, 6189.
[40] X. L. Wu, G. G. Siu, C. L. Fu, H. C. Ong, *Appl. Phys. Lett.* **2001**, *78*, 2285.
[41] C. Gaspar, F. Costa, F. Monteiro, *J. Mater. Sci.* **2001**, *12*, 269.
[42] H. J. Egelhaaf, D. Oelkrug, *J. Cryst. Growth* **1996**, *161*, 190.
[43] W. S. Shi, O. Agyeman, C. N. Xu, *J. Appl. Phys.* **2002**, *91*, 5640.
[44] J. Q. Hu, Y. Bando, *Appl. Phys. Lett.* **2003**, *82*, 1401.
[45] A. van Dijken, E. Meulenkamp, D. Vanmaekelbergh, A. Meijerink, *J. Phys. Chem. B* **2000**, *104*, 1715.
[46] A. van Dijken, E. Meulenkamp, D. Vanmaekelbergh, A. Meijerink, *J. Lumin.* **2000**, *90*, 123.
[47] S. C. Lyu, Y. Zhang, H. Ruh, H.-J. Lee, H.-W. Shim, E.-K. Suh, C. J. Lee, *Chem. Phys. Lett.* **2002**, *363*, 134.
[48] L. Dai, X. L. Chen, W. J. Wang, T. Zhou, B. Q. Hu, *J. Phys. Condens. Matter* **2003**, *15*, 2221.
[49] S. Mahamuni, K. Borgohain, B. S. Bendre, V. J. Leppert, S. H. Risbud, *J. Appl. Phys.* **1999**, *85*, 2861.
[50] Y. Dai, Y. Zhang, Q. K. Li, C. W. Nan, *Chem. Phys. Lett.* **2002**, *358*, 83.
[51] S. Monticone, R. Tufeu, A. V. Kanaev, *J. Phys. Chem. B* **1998**, *102*, 2854.
[52] M. H. Huang, Y. Wu, H. Feick, N. Tran, E. Weber, P. Yang. *Adv. Mater.* **2001**, *13*, 113.
[53] B. D. Yao, Y. F. Chan, N. Wang, *Appl. Phys. Lett.* **2002**, *81*, 757.
[54] J. Zhang, W. Yu, L. Zhang, *Phys. Lett. A* **2002**, *299*, 276.
[55] B. Lin, Z. Fu, Y. Jia, *Appl. Phys. Lett.* **2001**, *79*, 943.
[56] Z. Y. Xue, D. H. Zhang, Q. P. Wang, J. H. Wang, *Appl. Surf. Sci.* **2002**, *195*, 126.
[57] J. Q. Hu, X. L. Ma, Z. Y. Xie, N. B. Wong, C. S. Lee, S. T. Lee, *Chem. Phys. Lett.* **2001**, *344*, 97.

[58] X. L. Xu, S. P. Lau, J. S. Chen, G. Y. Chen, B. K. Tay, *J. Cryst. Growth* **2001**, *223*, 201.
[59] P. S. Xu, Y. M. Sun, C. S. Shi, F. Q. Xu, H., B. Pan, *Nucl. Instrum. Methods Phys. Res., Sect. B* **2003**, *199*, 286.
[60] F. Oba, S. R. Nishitani, S. Isotani, H. Adachi, I. Tanaka, *J. Appl. Phys.* **2001**, *90*, 824.
[61] M. H. Sukkar, K. H. Johnson, H. L. Tuller, *Mater. Sci. Eng. B* **1990**, *6*, 49.
[62] S. B. Zhang, S.-H. Wei, A. Zunger, *Phys. Rev. B* **2001**, *63*, 075205.
[63] A. F. Cohan, G. Ceder, D. Morgan, C. G. Van de Walle, *Phys. Rev. B* **2000**, *61*, 15 019.
[64] G. D. Mahan, *J. Appl. Phys.* **1983**, *54*, 3825.
[65] D. C. Look, J. W. Hemsky, J. R. Sizelove, *Phys. Rev. Lett.* **1999**, *82*, 2552.
[66] N. O. Korsunska, L. V. Borkovska, B. M. Bulakh, L. Yu. Khomenkova, V. I. Kushnirenko, I. V. Markevich, *J. Lumin.* **2003**, *102–103*, 733.
[67] V. A. L. Roy, A. B. Djurišić, W. K. Chan, J. Gao, H. F. Lui, C. Surya, *Appl. Phys. Lett.* **2003**, *83*, 141.
[68] W. Göpel, *J. Vac. Sci. Technol.* **1978**, *15*, 1298.
[69] C. G. Van de Walle, *Physica B* **2001**, *308–310*, 899.
[70] W. Hirschwald, P. Bonasewicz, L. Ernzt, M. Grade, D. Hoffmann, S. Krebs, R. Littbarski, G. Neumann, M. Grunze, D. Kolb, H. J. Schulz, in *Current Topics in Materials Science*, Vol. 7 (Ed: E. Kaldis), North-Holland, Amsterdam, The Netherlands **1981**, Ch. 3.
[71] A. B. M. Almamun Ashrafi, I. Suemune, H. Kumano, S. Tanaka, *Jpn. J. Appl. Phys., Part 2* **2002**, *41*, L1281.
[72] N. Ohashi, T. Ishigaki, N. Okada, T. Sekiguchi, I. Sakaguchi, H. Haneda, *Appl. Phys. Lett.* **2002**, *80*, 2869.
[73] C. G. Van de Walle, *Phys. Rev. Lett.* **2000**, *85*, 1012.
[74] A. Wood, M. Giersig, M. Hilgendorff, A. Vilas-Campos, L. M. Liz-Marzán, P. Mulvaney, *Aust. J. Chem.* **2003**, *56*, 1051.
[75] M. Oku, *Jpn. J. Appl. Phys., Part 1* **1993**, *32*, 4377.
[76] F. D. Auret, S. A. Goodman, M. J. Legodi, W. E. Meyer, D. C. Look, *Appl. Phys. Lett.* **2002**, *80*, 1340.
[77] W. Göpel, U. Lampe, *Phys. Rev. B* **1980**, *22*, 6447.

